

Synthesis and Size Control of Polystyrene Latices via Polymerization in Microemulsion

Markus Antonietti,* Wolfgang Bremser, Dorothea Müschenborn, Christine Rosenauer, and Beate Schupp

Institut für Physikalische Chemie der Universität Mainz, Jakob Welder Weg 15, D-6500 Mainz, West Germany

Manfred Schmidt

Max-Planck Institut für Polymerforschung, Ackermannweg 11, D-6500 Mainz, West Germany

Received March 4, 1991; Revised Manuscript Received July 17, 1991

ABSTRACT: This publication describes the controlled synthesis of very fine polystyrene latices with $10 \text{ nm} < R < 60 \text{ nm}$ via polymerization in microemulsion and their characterization by light- and neutron-scattering and electron microscopy. The microemulsions are formed by dispersion of styrene in water, using cetyltrimethylammonium chloride (CTMA) or dodecyltrimethylammonium bromide (DTMA) as surfactants. The size of the resulting particles is controlled only by the ratio of styrene to surfactant. Within a certain range, the relation between stoichiometry and droplet size is described by a simple geometric model. The limited pliability of the surfactant interface results in a minimum droplet size which is obtained at the limit of high surfactant concentrations. These particles, once polymerized, swell homogeneously with additional monomer. The geometric model for droplet size control can be generalized to other nonpolar monomers. By contrast, the polymerization in microemulsion of polar monomers such as methyl methacrylate (MMA) and even copolymerization reactions with MMA become more complex, and the simple model fails. We assume that MMA itself acts as a cosurfactant (self-surfacting system) and diminishes the interface energy in the case of copolymerization with styrene.

(I) Introduction

In 1943, Schulman and co-workers first described a transparent system which formed spontaneously upon the mixture of oil and water with surfactants.¹ The notation "microemulsion" for these systems was introduced in 1959 by the same authors.²

Despite the simplicity of this observation, no precise or commonly accepted definition of microemulsion exists (see also the arguments presented in ref 3). On the one hand, microemulsions must be differentiated from micellar solutions, and some groups name the systems presented below "swollen micelles". On the other hand, a wide variety of apparently similar systems is included in the phenomenologic definition of microemulsion, and dispersions obeying the same physical rules but exhibiting larger characteristic lengths (and a turbid appearance) are arbitrarily excluded.

In this paper we use the notation "microemulsion" for all dispersions of two separated and well-defined phases stabilized by interfacial surfactant layers, where the droplet size or characteristic length is a thermodynamically controlled equilibrium property. For practical reasons, the droplets should be small enough to prevent sedimentation within the time range of our experiments.

The performance of polymerization reactions in microemulsions can be used to obtain very small polymer particles on the order of the primary micelle size. It has been only 10 years since the first publications concerning such polymerization techniques appeared. Candau and Leong et al. have studied the polymerization of acrylamide in inverse microemulsion.⁴⁻⁷ They obtained dispersions with a low intrinsic viscosity.

Atik and Thomas polymerized styrene in an oil/water microemulsion^{8,9} and obtained narrowly distributed latex particles with diameters on the order of 20–30 nm. Their system, however, is based on hexanol as a cosurfactant, and it is known that the stability of such microemulsions

is limited by the solubility of the formed polymer in the cosurfactant.¹⁰ If copolymerization with a cross-linking agent is preformed in such systems, the network topology is also severely changed.¹¹

Johnson and Gulari performed light-scattering experiments on a similar microemulsion¹² before and after polymerization. They determined a bimodal distribution of their product and obtained no clear relation between droplet size and the molecular weight of the polymer.

Turro and El-Aasser et al. examined the photoinitiated polymerization of styrene in microemulsion, using pentanol as a cosurfactant and toluene as a mediator.¹³ They found that the latex size is slightly larger than the droplets of the corresponding microemulsion and almost independent of the initiation rate.

Jayakrishnan and Shah first demonstrated that the polymerization of styrene in microemulsion can be performed by surfactants alone, without a cosurfactant.¹⁴ Most recently, Thomas et al. published a recipe which also produces a microemulsion without a cosurfactant.¹⁵ They claim that the size of the resulting latex can be controlled by the amount of initiator, in contrast to the system described by Turro and El-Aasser. The smallest particles which Thomas et al. synthesized have a diameter of about 5.4 nm.

During recent investigations, we have used polymerization in microemulsions for the controlled synthesis of spherical microgels.¹⁶ In particular, we found that the relationship between the amount of surfactant and the resulting droplet or microgel size is not well established.

Such a relationship would allow for the controlled synthesis of ultrafine latex particles or microgels ($15 < d < 100 \text{ nm}$), materials with widespread technical and medical application (see, for instance refs 17–19). These sizes are clearly not within the range of standard emulsion polymerization techniques, which are limited to particles with diameters above 30 nm. For further comparison of

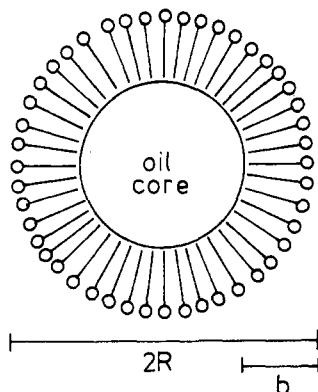


Figure 1. Idealized micelle structure. The spherical micelle with a radius R consists of an inner oil core and a surfactant layer with thickness b . All interphases are assumed to be sharp.

the possibilities and limitations of emulsion and microemulsion polymerization, the reader is referred to the extensive literature (e.g., refs 3, 20, and 21).

No general relationship exists, however, between latex size and stoichiometry for polymerization in microemulsion, since the size does not depend only on the monomer, initiator, and surfactant used. In some cases, effects of initiator concentration, temperature, and the kinetics of monomer exchange between the micelles are also reported.

The first part of this paper deals with a very simple case: the dispersion of styrene in each of two similar surfactants, cetyltrimethylammonium chloride (CTMA) and dodecyltrimethylammonium bromide (DTMA). Both form stable microemulsions of styrene in water without the aid of a cosurfactant.

Within the micelles of the microemulsions, we synthesize microgels by a cross-linking copolymerization of styrene and *m*-diisopropenylbenzene. The synthesis of microgels rather than linear polymers is advantageous in that the oil core polymerizes to one polymer molecule (the "microgel" particle). These microgels are easy to handle and keep their properties during precipitation and redissolution, as has been shown in ref 16. The isolation and characterization of the pure microgels therefore allow for direct conclusions about the structure and size of the inner oil core, alone.

Both latices and microgels are characterized by static and dynamic light scattering and electron microscopy. The combination of these techniques allows an accurate determination of the size, shape and polydispersity of the particles. All data will be related to a geometric model which predicts the latex size as a function of the amount of surfactant. It will be shown that this model agrees with the data for microemulsions of nonpolar monomers.

Since we are interested in the synthesis of latices with a more complex inner structure, the swelling behavior of the polystyrene latex is characterized. In addition, we examine whether or not the presented model is also valid for microemulsions of polar monomers such as MMA or mixed systems where the oil phase is formed by styrene and a minor amount of MMA.

(II) General Considerations

(II.1) Simple Model for the Structure of Spherical Microemulsions. In this paragraph, we present a simplified picture of the structure of a microemulsion. In the experimentally investigated composition range (oil content less than 30%), we usually expect the oil droplets to be spherical and suspended in the water phase. We also assume that the distribution of droplet sizes is uniform and that all surfactant molecules are located at the

interface between the oil and water phases. This approach neglects the presence of free surfactant molecules or empty micelles dissolved in the water phase and the existence of monomer droplets on the scale above $1\ \mu\text{m}$.

Such a picture is realistic if the main driving force for formation of the microemulsion is the minimization of the interface energy between oil and water; the bending energy of the interface layer is considered to be a minor effect.

With the additional assumption that the oil and water phases and the intermediate surfactant layer are separated by sharp boundaries, the droplet size is determined by simple geometrical arguments, sketched in Figure 1.

A micelle of radius R consists of an inner oil core surrounded by a spherical shell of surfactant with average thickness b . The macroscopic weight ratio of surfactant to monomer, S , is reflected in the volume ratio of oil core to covering surfactant for each droplet. We derive eq 1:

$$S = \frac{m_{\text{surf}}}{m_{\text{oil}}} = \frac{\rho_{\text{surf}}}{\rho_{\text{oil}}} \frac{(4/3)\pi R^3 - (4/3)\pi(R-b)^3}{(4/3)\pi(R-b)^3} \approx \frac{R^3}{(R-b)^3} - 1 \rightarrow R \approx b(1 - (1+S)^{-1/3})^{-1} \quad (1)$$

ρ_{surf} and ρ_{oil} are the densities of the surfactant and oil phases, respectively. We obtain a relationship between the relative composition and the radii of the micelles where the slope is given by the layer thickness. This equation has already been presented in ref 16. For a monolayer, the layer thickness is assigned to the geometrical length of the surfactant molecule.

We cannot expect, however, that this simple model holds for all polymerization reactions in microemulsion. On the one hand, it is assumed that the system has a minimum amount of free energy when the soap molecules in the interface are densely packed and the coverage is complete. This is only valid for surfactants with an apparently strong lateral attraction. Interface structures are known,³ however, which exhibit much smaller interface densities of surfactant molecules. At the end of this paper some real systems that deviate from the densely packed structure are shown. Such a behavior results in smaller particles than expected.

On the other hand, the surfactant molecules can build an interface which is thicker than a monolayer. Here, larger micelles than predicted by the simple model are obtained. This behavior is seen especially in the case of polymeric surfactants, and b is an increasing function of S (see ref 16).

Larger particles than predicted are also obtained when the microdroplets grow during polymerization. This is probably caused by a difference in interface energies between monomer/surfactant and polymer/surfactant or by a growth of the polymer chain through the micellar interfaces. Such behavior is known from the polymerization of acrylamide in inverse microemulsions, where the final latex results from the fusion of 60–150 primary micelles.⁷

For these reasons, we relate all experimental data to the geometrical model and calculate an apparent layer thickness b_{app} . From the comparison of b_{app} with the geometric length of the surfactant we obtain information about the interface structure and possible droplet aggregation.

(II.2) Swelling of Polymerized Microemulsions. If the above-described picture is realistic, we can also describe complex cases of two-step processing in microemulsion polymerization. From a practical point of view, these techniques represent possible starting points for the synthesis of more complicated polymer structures and

extend the potential applications of polymerization in microemulsion.

One may use the latices described in the previous section as a seed latex for a subsequent second polymerization step (performed by polymerization in microemulsion or in conventional emulsion). Alternatively, one can swell the particles immediately with a different monomer or monomer mixture, thus resulting in interpenetrating microgels or structured microgels. The synthesis and behavior of these structures will be presented in a forthcoming paper.

In the present paper, we only describe the elementary step of these applications, the swelling of the micelles. If we add the same monomer to a parent, polymerized microemulsion, three different scenarios can be expected:

(1) The new monomer will be unable to swell the micelles, since they are too stable. Monomer droplets will coexist with the old micelles.

(2) Surfactant and new monomer will form more stable micelles. The primary polymer will precipitate.

(3) The new monomer will enter the micelles and swell all of them at the same rate. Since the number of micelles and the amount of surfactant are fixed, the swelling will result in an interface where the surfactant density is lower. We call this state "incompletely covered". However, the interface energy increases with decreasing coverage. A homogeneous swelling process is most favorable.

It is obvious that structured systems can be synthesized only when the third scenario takes place. This case would also represent a means to form microparticles with well-defined surfactant coverages. It must be emphasized that the constraint of a constant particle number results in interface structures with higher energy (as compared to their previous minimum energy). This higher state of energy is, however, the minimum free energy of the new complete microemulsion.

(III) Experimental Section

(III.1) Polymer Synthesis. For a typical polymerization reaction in microemulsion, 10 g of freshly distilled styrene, the designated amount of cross-linker (e.g., 0.38 g *m*-diisopropenylbenzene (*m*-DIB) for a cross-linking density $p_c = 1/10$ or one cross-link per 10 monomer units), and 50 mg of a lyophilic initiator such as AIBN (azobisisobutyronitrile) are mixed to form the oil phase. The solution of the calculated amount of surfactant (e.g., 10 g of DTMA (Aldrich) or CTMA (Merck)) in deionized and degassed water is prepared separately (100 g altogether). The oil and water phases are dispersed with a high-speed stirrer and are then stirred for 16 h at room temperature. The reaction mixture is heated afterward to 60–70 °C. The reaction is completed after 72 h; the conversion depends on the droplet size and typically exceeds 80% in the case of the smaller microgels and 95% in the case of the largest droplets, as determined by the mass of isolated polymer.

An aliquot of the product is kept for characterization of the latex by electron microscopy and dynamic light scattering, and the remaining portion is precipitated by addition of 200 mL of hot methanol. The surfactants have to be carefully removed from the microgels by a 3-fold reprecipitation.

Here, the crude product is redissolved in 100 mL of THF and precipitated in 500 mL of methanol by dropwise addition of the microgel solution. After this procedure, no surfactant can be detected in the microgel samples by chloride (bromide) analysis.

The resulting white powder is dried in the vacuum oven for 48 h at 50 °C.

(III.2) Static and Dynamic Light Scattering. After completion of the polymerization reaction, the latices are characterized by light scattering in water at 20 °C. The spectrometer and procedure for simultaneous static and dynamic light scattering are described in the literature.²² The measure-

ments are performed at 647.1 nm by means of a krypton ion laser (Spectra-Physics 2025).

The latex dispersions are optimized for the light-scattering experiments by diluting the crude concentrated reaction product with an excess of deionized water until the count rate of the resulting mixture is within the optimal range of the spectrometer. These dilute solutions are purified by filtering them through Millipore HA 0.45- μ m filters.

The final concentrations typically range between 1 and 10⁻² g/L and can be estimated from the concentration of the primary microemulsion. Since we are only interested in the hydrodynamic radius and the radius of gyration of the latex particles, the absolute scattering intensity is not quantitatively evaluated. The characterization of the microemulsion by light scattering prior to polymerization fails. This is possibly caused by the significant solubility of styrene in water which destabilizes the micelles.

In some cases, the resulting microgels are also characterized in a toluene solution at 20.0 °C. In these experiments, we follow exactly the route described in our earlier work dealing with the behavior of spherical microgels.¹⁶

(III.3) Small-Angle Neutron Scattering. The small-angle neutron-scattering experiments (SANS) are carried out at the Institut Laue-Langevin in Grenoble, France, using the small-angle diffractometers D17 and D11.²³ The measurements on the D17 are performed using sample-to-detector distances of 1.2, 2, and 3.45 m and incident neutron wavelengths of $\lambda = 1.2$ nm and $\lambda = 1.8$ nm. The measurements on the D11 are made with wavelengths of $\lambda = 0.6$ nm and detector and distances between 2.5 and 36 m. The distribution of wavelengths $\Delta\lambda/\lambda$ is below 10% on both instruments. The preparation of the samples and the further treatment of the scattering data are analogous to the procedure applied to the characterization of DVB microgels.²⁴

(III.4) Electron Microscopy. All measurements are performed with a Phillips 3000 electron microscope. The polymerized microemulsions are diluted with distilled water to a latex content of 0.1%, and the mixture is stirred for 3 min in an ultrasonic bath. A droplet of this sample is rinsed over a carbonized copper grid, and the water is allowed to evaporate. The resulting deposits are shadowed with Pt/C at an angle of 20°.

(IV) Results and Discussion

(IV.1) Microemulsions with Styrene. The microemulsions, once polymerized, remain stable at least over 2 years. Systems with the surfactants CTMA and DTMA and *S* ratios larger than $S = 1.5$ are translucent or transparent. All other systems are opaque, due to the formation of larger micelles. Optical micrographs of all microemulsions from this investigation taken with a dark-field condenser before and after the polymerization clearly indicate the absence of monomer droplets or polymer particles with sizes greater than 1 μ m. This proves that the polymerization occurs neither as an emulsion polymerization nor in a two-phase region with a coexisting microemulsion phase.

The viscosity of the microemulsions formed by CTMA and DTMA is close to that of water, which indicates a spherical geometry of the micelles.

Figure 2 shows the optical transmission of two selected samples (CTMA/4 and CTMA/2) as a function of the polymerization time *t*. These values are determined with a conventional UV-vis spectrometer at 700 nm in a cuvette with an optical length of 1 cm. The gap at the beginning of the curves represents the change of turbidity during the 16 h of stirring before the start of the reaction.

We observe that the transmission clearly decreases during this waiting time, indicating a relatively slow approach to equilibrium. The decrease in turbidity is caused either by a decrease in the average micelle size or by a narrowing of the micelle size distribution which allows for a better packing of the micelles. The turbidity increases only slightly during the reaction and is approximately

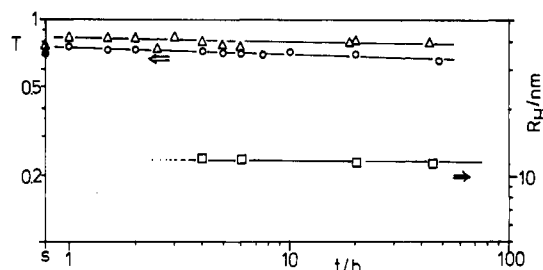


Figure 2. Optical transmission T in dependence of the polymerization time t for the samples DTMA/4 (Δ) and DTMA/2 (O). For DTMA/2, also the hydrodynamic radius of the latices is presented (\square).

Table I
Characterization of the Latex after Polymerization^a

sample	S	$r_H(\text{latex})/\text{nm}$	u_2	b_{app}/nm
CTMA/0.2	0.2	54.3		3.2
CTMA/0.4	0.4	31.9	0.077	3.4
CTMA/0.5a	0.5	26.3	0.062	3.3
CTMA/0.5b	0.5	25.3	0.056	3.2
CTMA/1	1.0	16.4	0.093	3.4
CTMA/2	2.0	13.1	0.099	4.0
CTMA/3.3	3.3	10.5	0.108	4.0
DTMA/0.2	0.2	60.3	0.073	3.6
DTMA/0.25	0.25	46.0	0.060	3.3
DTMA/0.35	0.35	32.5	0.052	3.1
DTMA/0.5a	0.5	23.5	0.064	3.0
DTMA/0.5b	0.5	24.7	0.038	3.1
DTMA/0.6	0.6	23.6	0.036	3.4
DTMA/0.8a	0.8	21.3	0.056	3.8
DTMA/0.8b	0.8	20.3	0.048	3.6
DTMA/1	1.0	16.5	0.041	3.4
DTMA/1.5	1.5	17.1	0.061	4.5
DTMA/2	2.0	12.3	0.036	3.8
DTMA/3.5	3.5	9.1	0.055	3.6
DTMA/4	4.0	10.8	0.090	4.5

^a r_H is the hydrodynamic radius of the latex after polymerization as determined by dynamic light scattering, u_2 the normalized second cumulant at 90° scattering angle, and b_{app} the apparent layer thickness as calculated from eq 1. CTMA and DTMA are the surfactants used.

described by the change in the index of refraction due to polymerization, only.

Figure 2 also presents the hydrodynamic radii of the diluted latex of sample CTMA/2 at different stages of reaction, as determined by dynamic light scattering. The characterization of the primary, nonpolymerized microemulsion in dilution fails. After formation of a small amount of polymer (about 20%), the latex becomes stable to dilution, and a hydrodynamic radius can be determined from the experiments. This radius does not depend on the polymerization time or the extent of reaction.

Both sets of experiments clearly show that the micelles maintain a constant size during polymerization and do not grow.

In Table I, the hydrodynamic radii of the latices after polymerization are related to different amounts of the surfactants DTMA and CTMA. For most cases, the normalized second cumulants (from the dynamic light-scattering experiments at a 90° scattering angle) as a measure of the polydispersity of the particles are given. In general, DTMA produces micelles which are less polydisperse than the corresponding CTMA micelles. All size distributions are relatively small and are estimated from the data to have polydispersity indices of $R_w/R_n < 1.05^{11}$ (we follow a procedure described in ref 28).

The droplet sizes for both series are controlled only by the amount of surfactant and can in principle be controlled to give radii between $10 \text{ nm} < R < 60 \text{ nm}$. Compared to the data from a microemulsion using a polymeric surfac-

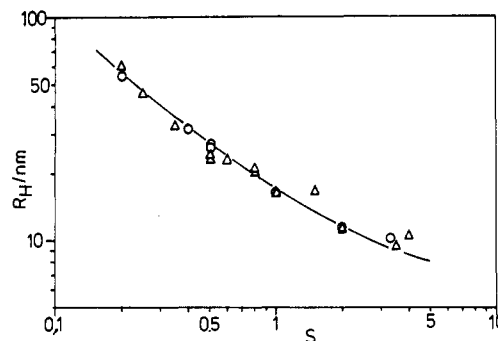


Figure 3. Hydrodynamic radius r_H of the latices in dependence of the relative amount of surfactant S for DTMA (Δ) and CTMA (O). The straight line represents the calculated behavior corresponding to eq 1 and an interlayer thickness $b = 3.5$.

tant,¹⁶ these data demonstrate a significant extension of the accessible micelle size toward smaller values. A variation of the initiator concentration at three different amounts of surfactant clearly did not change the latex size.

We have not extended our investigations to S ratios smaller than 0.2. In these systems, the micelles become more polydisperse with a decreasing amount of surfactant, and the whole mixture becomes unstable at still lower S values. Most probably, we have reached the limit of solubilization for this specific monomer/surfactant system. In this regime, we also expect the transition from polymerization in microemulsion to the conventional polymerization in emulsion or miniemulsion.²⁷

A more quantitative relationship is given in Figure 3, which shows the hydrodynamic radii of the surfactant-stabilized micelles as a function of S . The straight line results from the simple micelle model introduced above with a fitted apparent layer thickness $b = 3.5 \text{ nm}$. We observe that within experimental error the latex size dependence for both surfactants is described well by this simple model. Systematic deviations are seen only for very small spheres. Here, the micelles become larger than expected, corresponding to a larger apparent layer thickness. We relate this deviation to the limited bending flexibility of the surfactant layer; it is obviously more favorable to produce larger droplets with a less defined interface structure than to produce smaller micelles. All attempts to produce droplets with still smaller radii than shown in Figure 3 have failed.

We observe practically no influence of the surfactant chain length (C_{12} and C_{16}). This proves the absence of an influence of surfactant solubility, since the critical micelle concentrations of these surfactants differ by 2 orders of magnitude. The latex size is, within certain limits, also not influenced by the size and polarizability the counterion (Br^- and Cl^-).

The measured apparent layer thickness $b = 3.5 \pm 0.4 \text{ nm}$ (as taken from the straight line) is slightly larger than the geometric length of the surfactants in the all-trans form of approximately 2.7 nm (CTMA) or 2.3 nm (DTMA). With respect to the Gouy-Chapman layer and the hydrodynamically active hydration shell of the polar end, the difference falls within a reasonable range.

Using the same simple geometric model, it is also possible to calculate for the interlayer the surface area A per surfactant molecule. We obtain an experimental value of about 0.14 nm^2 . This value is significantly below the value known for the densely packed state of monofunctional surfactants, $A \approx 0.18 \text{ nm}^2$.²⁹ Within the examined microemulsions, the geometry of the surfactant phase is apparently thicker and less defined than a monolayer. The

Table II
Data for Different Microgels in Toluene at 20.0 °C^a

sample	p_c	M_w	r_G/nm	r_H/nm	u_2	P	R_{HC}/nm	b'_{app}/nm
CTMA/3.3	1/10	4.82×10^6 4.4×10^6 ^b	5.5 ^b	8.9	0.032	0.62	7.1	3.4
CTMA/1	1/10	2.95×10^6	(14.6)	16.3	0.032	(0.90)	12.2	4.2
DTMA/0.8a	1/20	9.63×10^6	21.5	28.9	0.029	0.74	16.0	5.3
DTMA/0.8b	1/40	10.0×10^6	26.5	34.2	0.028	0.78	16.2	4.1
DTMA/0.6	1/60	17.9×10^6	31.2	40.7	0.023	0.79	19.7	3.9
DTMA/0.5b	1/80	21.8×10^6	32.6	42.3	0.025	0.77	21.0	3.7
DTMA/0.25	1/80	217×10^6	81.6	105.8	0.018	0.77	43.4	2.6

^a Notation of symbols: p_c , cross-linking density; M_w , molecular mass determined with light scattering; r_H , hydrodynamic radius of the swollen microgel; u_2 , normalized second cumulant; r_G , radius of gyration; $P = r_G/r_H$; R_{HC} , hard-core radius as calculated from M_w ; b'_{app} , apparent layer thickness as calculated from the difference of R_{HC} and r_H (latex). ^b Determined with small-angle neutron scattering.

successful description of the relation between size and stoichiometry with one effective layer thickness, however, indicates that the surfactant distribution between the phases changes just slightly with changing S and droplet size.

Since we have performed a cross-linking copolymerization in these microemulsions, we can also examine the structure of the oil cores of the micelles. We carefully remove the surfactant as described above and examine the swollen microgels in solution. From the determined molecular weights we can calculate a hard-core diameter of the oil phase prior to swelling. This size is corrected with the extent of reaction.

In addition, we determine the P ratio ($P = r_G/r_H$) in the swollen state as a measure of the shape anisotropy or the radial density function of the microgels (for a further discussion of this point, see ref 16).

Table II shows these data for some selected microgels. The P values of about 0.76 for the larger particles indicate that these microgels are indeed spherical and homogeneously swollen. The smaller P value for the smallest microgel is probably due to the fact that r_H overestimates the particle radius on this size scale (here, the latex is only slightly larger than the solvent molecules). In addition, the scattering of the data in this region is generally quite high. From the normalized second cumulants we can deduce that the microgels are apparently less polydisperse than the parent microemulsion. This can only be interpreted by a small amount of temporary aggregates in the latex which would result in an apparent broadening of the micelle size distribution.

We calculate an interlayer thickness b' from the difference between the latex size and the hard-core radius, which is on the same order as b from the fitted geometric model.

It should be mentioned that the polydispersities of very small microgels are larger than those of the bigger particles, as reflected in the second cumulants of both latices and microgels. We have not yet clarified whether or not this behavior results from a broader droplet distribution of the parent microemulsion or from a small amount of agglomerates formed during polymerization.

The microgel cores can also be characterized by small-angle neutron scattering.

Figure 4 presents the master curves of the absolute scattering cross section of sample A50a¹⁶ in toluene, which is representative for all larger microgels. Five different detector distances between 2.5 and 36 m on D11 are superimposed in order to obtain scattering intensities over a wide range of the scattering vector Q . The same set of data is plotted in three different presentations: a double-logarithmic plot, a logarithmic Kratky plot, and a logarithmic Porod plot.

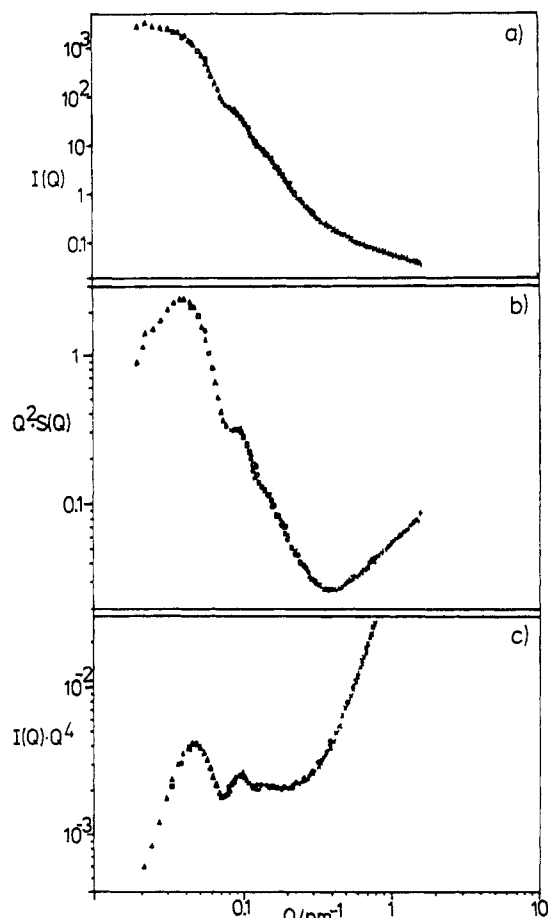


Figure 4. Master curve of the absolute scattering cross section of sample A50a as determined by SANS. The same set of data is presented in three different ways: (a) a double-logarithmic plot; (b) a Kratky plot; (c) a Porod plot.

We observe that the scattering behavior of microgels evidently follows the form factor of a sphere. The occurrence of typical oscillations in the form factor (best seen in the Porod presentation) can be regarded as a measure for the moderate polydispersity of the spheres. A fit of the experimental data with the theoretical curve results in a molecular weight of about $M_w \approx 186 \times 10^6$ and a radius of gyration of 55 nm. These data agree with the results of the static light-scattering experiment (given in ref 16).

At Q values larger than 0.5 nm^{-1} , the scattering behavior is dominated by the local structure of the microgels, which is similar to that of a polymeric network. In other words, this Q range allows us to observe the spatial correlation between the network meshes. In this work we are interested in the global structure only, and we will not perform further analysis of this part of the scattering curve.

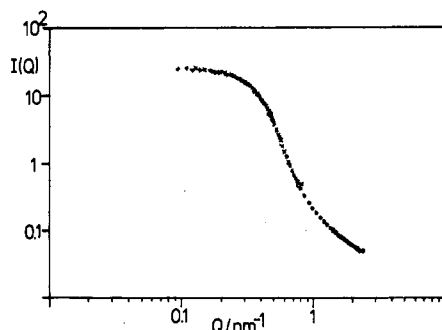


Figure 5. Master curve of the SANS data of sample DTMA/4.

The scattering profiles of very small microgels differ from the ideal shape of the monodisperse sphere, as exemplified in Figure 5 (sample DTMA/4). Although we observe the classical Q^{-4} profile of a massive three-dimensional body with a sharp surface, the oscillations of a sphere are not visible. We can interpret this as a relatively high polydispersity of the particles ($M_w/M_n > 1.2$) or as a nonspherical microgel structure in the swollen, dissolved state. At least, we can determine from this master curve the molecular weight and radius of gyration of the sample (included in Table III).

In addition, the structure of the polymerized cores at the limit of high surfactant concentrations is severely influenced by a phenomenon we call the "finite size effect". We have to consider that each primary micelle is very small and consists of only about 6400 surfactant molecules, 4500 monomer units, 225 cross-linker molecules, and 14 starter molecules (for $S = 4$ and $p_c = 1/10$). These values are so small that fluctuations of the composition or the extent of reaction in each micelle may result in a more polydisperse distribution of microgel structures than is represented by the micelle size alone. Since the average number of consecutive cross-links in each spatial direction is only about six, each microgel may also swell heterogeneously (from a sphere to a "potato"). This would explain the absence of oscillations in the structure factor.

Unfortunately, the performance of high-resolution GPC on the microgels in the swollen state fails. A strong absorption interferes with the separation with respect to the hydrodynamic volume. We can only estimate an upper limit for the polydispersity which is about $M_w/M_n \approx 1.2$ for sample DTMA/4. A more detailed discussion of the GPC/LS experiments of such highly cross-linked structures will be the subject of a forthcoming publication.²⁵

A method for the direct determination of particle size, shape, and polydispersity is electron microscopy. We were unable, however, to prepare samples with sufficient contrast for the observation of microgels without surfactant; only the primary latex could be characterized.

Usually, one observes strictly spherical particles which are moderately polydisperse. A histographical evaluation of such micrographs (with hundreds of particles) results in polydispersities of $1.01 < d_w/d_n < 1.05$.^{11,26} Also with electron microscopy, we observe a tendency toward higher polydispersities when the particles become smaller. Also the average size of the particles excellently corresponds to the values determined by dynamic light scattering of the latex. We conclude that electron microscopy confirms our description of the structure of microemulsion latices based on styrene.

(IV.2) Swelling Experiments on Microemulsion Latices. In these experiments, sample CTMA/0.35 is swollen with 30%, 50%, and 100% styrene (percentage with respect to the amount of monomer in the first polymerization step). After 24 h of equilibration, the samples

Table III
Characterization of a Microemulsion Latex Prior to and after Addition of Three Different Amounts of Monomer^a

sample	r_H /nm	u_2	Q_{mol}	C
DTMA/0.35	32.5	0.052		1
+50% styrene	37.0	0.047	1.54	0.75
+70% styrene	38.2	0.021	1.71	0.70
+100% styrene	41.7	0.042	2.28	0.58

^a r_H denotes the hydrodynamic radius of each latex, u_2 the normalized second cumulant, Q_{mol} the experimentally determined swelling ratio of the micelle cores, and C the resulting relative amount of surface coverage.

are polymerized for the second time. Dark-field micrographs indicate that no remaining monomer droplets or precipitated polymer is formed. We conclude, therefore, that the micelles do indeed swell. Table III shows the characterization of the swollen latices by dynamic light scattering after the second polymerization step.

From the ratio of the hydrodynamic radii of the swollen and unswollen latex particles, we can calculate the molecular swelling ratio Q_{mol} of each micelle core. We observe that, within experimental error, the micelles swell as expected from the amount of added monomer. The polydispersities of the dispersions also remain small, as indicated by the normalized second cumulants. These facts demonstrate indirectly that the swelling process occurs homogeneously.

Since it is assumed that the surface of the primary latex is covered by a densely packed monolayer of surfactant molecules, a parameter C is calculated which describes the lower relative surface coverage by the surfactant. Physically, this lower coverage results either in empty spots in the layer or in a looser packing of the surfactant molecules ("liquidlike" interface), depending on the surfactant.

In the present data set, dispersed particles with $C = 0.58$ are still stable. It must be emphasized that 0.58 is not the minimum value for a stable latex with these surfactants. Swelling ratios of larger than 100% were not investigated but can in principle be performed.

(IV.3) Microemulsions with Other Monomers. We have demonstrated that the dispersions presented here are also stable when the surface coverage of the particles by the surfactant molecules is incomplete. This behavior is universal; it holds for all latices resulting from emulsion polymerizations where also only a small part of the surface is stabilized by soap molecules.^{19,20} In addition, it is known from all classical microemulsions supported by a cosurfactant that a lower interfacial energy between the oil and water phases supports the formation of smaller micelles. These interfaces also do not consist of a densely packed surfactant monolayer.

From these facts we conclude that the accuracy of the simple model which describes the relationship between micelle size and relative amount of surfactant depends on the relationship between the cohesion energy of the interface layer and the interface energy between the oil and water phases. Therefore, it is not expected that the model can be generalized to all monomer/surfactant systems.

For the determination of the influence of the monomer, we have tried to create and polymerize microemulsions with four other monomers. We have chosen two amphiphilic monomers (methyl methacrylate and cyclohexyl methacrylate) because their polarity should influence the interface structure. We have also investigated the behavior of partially fluorinated monomers (*p*-fluorostyrene and

Table IV
Characterization of Latices Made of Monomers Other Than Styrene^a

monomer	<i>S</i>	<i>r_H</i> (meas)/nm	<i>r_H</i> (calc)/nm
4-fluorostyrene	1.0	17.6	17.0
cyclohexyl methacrylate	0.5	25.8	27.7
cyclohexyl methacrylate	2.0	13.2	11.4
MMA	0.1	18.9	(111.9)
MMA	0.2	25.3	59.4
MMA	0.5	15.5	27.7
90% styrene/10% MMA	0.5	19.6	27.7

^a The surfactant is in all cases CTMA. *S* is the relative amount of surfactant and *r_H*(meas) the experimentally determined hydrodynamic radius of the latices. *r_H*(calc) is the corresponding value as expected from the geometric model.

pentafluorostyrene), where we expect to decrease the compatibility of the oil phase and the surfactant.

For pentafluorostyrene, the polymerization in microemulsion failed. Although the microemulsion of the monomer is stable, the micelles agglomerate during the polymerization until macroscopic precipitation takes place. Only a minor mass fraction is still dispersed in water, most probably existing in a metastable state, only. We can interpret this behavior as an insufficient stabilization of the fluorinated, polymeric surface by the surfactant.

In the other three cases, the polymerization in microemulsion was successful with respect to the stability of the latex.

Table IV shows the data of these polymerized latices. For comparison, we have also included the calculated values for the latex size as expected from the geometric model with *b* ≈ 3.5 nm.

The polymerization of 4-fluorostyrene in microemulsion results in particles whose size agrees with the predicted values. Apparently, the proposed droplet and interface structure also holds for this monomer. By diminishing the number of fluorine substituents, we have increased the compatibility between polymer and surfactant. Consequently, the polymerized microemulsion remains stable. However, the concentration regime in which the polymerization in microemulsion actually occurs is more restricted (*S* ≥ 0.5), as deduced from experiments with smaller amounts of surfactant.²⁶ This can be explained by a higher solubilization limit of this monomer.

For methyl methacrylate, no relationship between the amount of surfactant and size of the latex can be found. The resulting particles are generally very small, and even pure MMA without surfactant can be polymerized, resulting in a latex of small size. In the latter case, the turbidity of the dispersion during polymerization decreases sharply. This indicates that (besides polymerization in microemulsion) a second polymerization mechanism exists which results in finely dispersed particles. This additional mechanism may be supported by the increased solubility of MMA in water which is five times larger than the corresponding one of styrene. This solubility is so large that we cannot even exclude polymerization in the aqueous phase (although a lyophobic initiator is used). We conclude that stabilization of MMA droplets by a surfactant is not sufficient to strictly control the latex structure.

If methyl methacrylate lowers the interface energy between the oil and water phases and acts therefore as a cosurfactant, the copolymerization of styrene and MMA in microemulsion should also result in particles which are smaller than pure polystyrene particles. The data for a monomer mixture consisting of 90% styrene/10% MMA in Table IV clearly support this expectation. For this

system, we calculate an apparent surface coverage by the surfactant of *C* ≈ 0.71, which may serve as a measure of the affinity of the MMA molecules to the interface.

This "self-surfacting" effect is less pronounced for cyclohexyl methacrylate (CMA). Here, the simultaneous increase of the hydrophobicity and the bulkiness of the side group prevents the incorporation of the monomer in the interface, at least at high relative surfactant concentrations. At small *S* ratios below *S* = 0.5, the PCMA latices become generally smaller than expected.

(V) Comparison to Other Experiments

We now relate these results to some controversial data for oil-in-water microemulsions found in the literature.

The latex synthesized by Atik and Thomas,^{8,9} using CTMA as a surfactant and hexanol as a cosurfactant, was only slightly smaller in diameter than the value determined for pure CTMA at the same *S* ratio (31 nm compared to 34 nm). This difference may originate from an insufficient contrast of the surfactant layer in electron micrographs, but can also be explained by the influence of the cosurfactant.

In a more recent work, Thomas et al. have also examined polymerized microemulsions of CTMA without cosurfactant.¹⁵ Their claim that the latex size depends on the amount of initiator clearly contradicts our experimental latex size control results. The smallest radius they obtained (*R* = 5.4 nm) is in a region where our micelles become unstable. No explanation for these differences can be given.

Jayakrishnan and Shah¹⁴ found that most experimental procedures using a nonsolvent such as hexanol become unstable during polymerization, in agreement with ref 10. Only a mixed surfactant system without a cosurfactant could produce shape. No absolute sizes are given in this paper. From microemulsion with extremely small particles which were nonspherical in kinetic observations they conclude that the microdroplets must be covered with a firm surfactant layer. This fact is in agreement with the area calculations according to our model.

Turro and El-Aasser et al.¹³ found that the droplets of a polymerized microemulsion (styrene/toluene/pentanol/sodium dodecyl sulfate/water) grow during polymerization. We attribute this behavior to the unknown effect of pentanol on the growing polymer particles, even in the presence of toluene. The particle diameter of the latex with the greatest conversion was 47 nm. Assuming that the simple model also holds for sodium dodecyl sulfate and neglecting the influence of pentanol on the final latex size, we would expect a diameter of 42 nm for *S* = 0.67.

El-Aasser and Vanderhoff et al. also examined very accurately the composition of oil, water, and surfactant interfaces by the combination of three different techniques.³⁰ Their results on the system styrene/pentanol/sodium dodecyl sulfate/water show that the styrene is mainly located in the oil core; only minor amounts of styrene are within the interface or the water phase. Oil and water mutually dissolve only up to the solubilization limit (0.03% and 0.3%, respectively). These facts show the restricted validity of a simplified description of a microemulsion as a mixed system with three moderately well-defined phases, at least for the prediction of simple relations as the composition size dependence.

(VI) Summary and Conclusions

We have demonstrated by means of the data presented above that microemulsions made of styrene-DTMA/CTMA-water behave ideally with respect to a very simple

geometric model. In this model, all surfactant molecules are located on the surface of spherical monomer droplets and form a well-defined interlayer. During polymerization, the droplet size does not change, at least within experimental accuracy. The size of the polymerized latices is quantitatively controlled by the amount of surfactant within a size range of $10 \text{ nm} < R < 60 \text{ nm}$. The synthesis of still smaller particles has failed, possibly due to the limited pliability of the surfactant layer. The latices are only moderately polydisperse ($d_w/d_n \leq 1.05$). Very small latex particles exhibit a tendency toward greater polydispersities.

Data reported in the literature for similar oil-in-water microemulsions agree with the observed behavior, at least qualitatively. A closer comparison is prohibited by the use of different surfactants and compositions in the investigated systems.

The primary latex particles can be further processed; they can be swollen with another monomer for instance. This swelling occurs homogeneously: each particle swells at the same rate, as detected by light scattering. Besides its application as a seeding latex, this behavior allows the construction of latex particles with a more complex architecture, e.g., interpenetrating microgels or hollow spheres. As a byproduct, well-defined nonideal surfactant layers are formed on the surface of the swollen particles.

The micelle size of microemulsions of 4-fluorostyrene and cyclohexyl methacrylate is also controlled by the amount of surfactant and parallels the behavior of the analogous styrene micelle size at S ratios larger than $S = 0.5$. By contrast, microemulsions of methyl methacrylate are composed of micelles which are much smaller than the corresponding micelles of nonpolar monomers. No size control of the latex can be obtained by altering the surfactant concentration. This behavior is explained by a self-surfacting effect in which MMA itself acts as a co-surfactant.

A similar behavior is seen in the copolymerization of styrene and MMA in microemulsion in which a latex is obtained with a diameter smaller than predicted. Since MMA is miscible with styrene and polystyrene, this technique represents an experimental route to smaller particles with smaller amounts of surfactant; this may have technological implications.

Acknowledgment. We thank H. Sillescu for many helpful comments and discussions. We are also indebted to P. Lindner and to I. Voigt-Martin for their competent help in context with neutron-scattering experiments and

electron microscopy. Financial support by the Deutsche Forschungsgemeinschaft is gratefully acknowledged.

References and Notes

- (1) Hoar, J. P.; Schulman, J. H. *Nature* **1943**, *152*, 102.
- (2) Schulman, J. E.; Stoeckenius, W.; Prince, L. *J. Phys. Chem.* **1959**, *63*, 1677.
- (3) Leung, R.; Jeng Hou, M.; Shah, D. O. *Surfactants in Chemical/Process Engineering*; Surfactant Science Series 28; Marcel Dekker: New York, 1988; p 315.
- (4) Leong, Y. S.; Riess, G.; Candau, F. *J. Chem. Phys.* **1981**, *78*, 279.
- (5) Candau, F.; Leong, Y. S.; Pouyet, G.; Candau, S. *J. Colloid Interface Sci.* **1984**, *101*, 167.
- (6) Candau, F.; Leong, Y. S. *J. Polym. Sci., Polym. Chem. Ed.* **1985**, *23*, 193.
- (7) Candau, F. *Encycl. Polym. Sci. Eng.* **1986**, *9*, 718.
- (8) Atik, S. S.; Thomas, J. K. *J. Am. Chem. Soc.* **1981**, *103*, 4279.
- (9) Atik, S. S.; Thomas, J. K. *J. Am. Chem. Soc.* **1982**, *104*, 5868.
- (10) Gan, L. M.; Shew, C. H.; Friberg, S. E. *J. Macromol. Sci., Chem.* **1983**, *A19*, 739.
- (11) Bremser, W. Diplomarbeit, Universität Mainz, 1988.
- (12) Johnson, P. L.; Gulari, E. *J. Polym. Sci., Polym. Chem. Ed.* **1984**, *22*, 3967.
- (13) Kuo, P. L.; Turro, N. J.; Tseng, C. M.; El-Aasser, M. S.; Vanderhoff, J. W. *Macromolecules* **1987**, *20*, 1216.
- (14) Jayakrishnan, A.; Shah, D. O. *J. Polym. Sci., Polym. Lett. Ed.* **1984**, *22*, 31.
- (15) Ferrick, M. R.; Murtagh, J.; Thomas, J. K. *Macromolecules* **1989**, *22*, 1515.
- (16) Antonietti, M.; Bremser, W.; Schmidt, M. *Macromolecules* **1990**, *23*, 3796.
- (17) Karamata, D. *J. Ultrastruct. Res.* **1971**, *35*, 201.
- (18) Ottewill, R. H.; Shaw, J. N. *J. Electroanal. Chem.* **1972**, *37*, 133.
- (19) Azad, A. R.; Ugelstad, J.; Fitch, R. M.; Hansen, F. K. *Emulsion Polymerization*; ACS Symposium Series 24; American Chemical Society: Washington, DC, 1976.
- (20) Piirma, I., Ed. *Emulsion Polymerization*; Academic: New York, 1976.
- (21) Shah, D. O., Ed. *Macro- and Microemulsion: Theory and Applications*; ACS Symposium Series 272; American Chemical Society: Washington, DC, 1985.
- (22) Bantle, S.; Schmidt, M.; Burchard, W. *Macromolecules* **1982**, *15*, 1604.
- (23) Neutron Research Facilities at the ILL High Flux Reactor, ILL, Grenoble, France, 1986.
- (24) Antonietti, M.; Rosenauer, C., submitted to *Macromolecules*.
- (25) Antonietti, M.; Schmidt, M., to be published.
- (26) Müschenborn, D. Diplomarbeit, Universität Mainz, 1990.
- (27) Rosen, M. J. *Surfactants and Interfacial Phenomena*; Wiley: New York, 1989.
- (28) King, T. A.; Treadaway, M. F. *J. Chem. Soc., Faraday Trans. 2* **1977**, *73*, 1616.
- (29) Tanford, C. *The Hydrophobic Effect*, 2nd ed.; Wiley: New York, 1980.
- (30) Guo, J. S.; El-Aasser, M. S.; Sudol, E. D.; Yue, H. J.; Vanderhoff, J. W. *J. Colloid Interface Sci.* **1990**, *140*, 175.

Registry No. CTMA, 112-02-7; DTMA, 112-00-5; *m*-DIB/styrene (copolymer), 26124-82-3; *m*-DIB/4-fluorostyrene (copolymer), 136893-19-1; *m*-DIB/CMA (copolymer), 136893-20-4; *m*-DIB/MMA (copolymer), 136893-21-5; *m*-DIB/MMA/styrene (copolymer), 136893-22-6.